WANL-PR(Q)-010

NASA-CR-72020

DEVELOPMENT OF DISPERSION STRENGTHENED TANTALUM BASE ALLOY

Ninth Quarterly Report

by

R.W. Buckman and R.C. Goodspeed

prepared for

National Aeronautics and Space Administration

Lewis Research Center

Space Power Systems Division

Under Contract (NAS 3-2542)

Astronuclear Laboratory

Westinghouse Electric Corporation

NOTICE

This report was prepared as an account of Government-sponsored work. Neither the United States nor the National Aeronautics and Space Administration (NASA), nor any person acting on behalf of NASA:

A) Makes any warranty or representation, expressed or implied, with respect to the accuracy, completeness, or usefulness of the information contained in this report, or that the use of any information, apparatus, method, or process disclosed in this report may not infringe privately-owned rights; or

B) Assumes any liabilities with respect to the use of, or for damages resulting from the use of any information, apparatus, method or process disclosed in this report.

As used above, "person acting on behalf of NASA" includes any employee or contractor of NASA, or employee of such contractor, to the extent that such employee or contractor of NASA or employee of such contractor prepares, disseminates, or provides access to, any information pursuant to his employment or contract with NASA, or his employment with such contractor.

Copies of this report can be obtained from:

National Aeronautics & Space Administration
Office of Scientific and Technical Information
Washington 25, D. C.
Attention: AFSS-A

Astronuclear Laboratory

WANL-PR-(Q)-010
NASA-CR-72020

DEVELOPMENT OF DISPERSION STRENGTHENED TANTALUM BASE ALLOY

by

R. W. Buckman, Jr.

and

R. C. Goodspeed

NINTH QUARTERLY PROGRESS REPORT

Covering the Period

November 20, 1965 to February 20, 1966

Prepared For

NATIONAL AERONAUTICS AND SPACE ADMINISTRATION
Contract NAS 3-2542

Technical Management
Paul E. Moorhead
NASA-Lewis Research Center
Space Power Systems Division

Astronuclear Laboratory
Westinghouse Electric Corporation
Pittsburgh 36, Pa.

TABLE OF CONTENTS

LIST OF TABLES

LIST OF ILLUSTRATIONS

FOREWORD

This report was prepared by the Westinghouse Astronuclear Laboratory under Contract NAS 3-2542. This work is administered under the direction of the Space Power Systems Division of the National Aeronautics and Space Administration with Mr. P. E. Moorhead acting as Technical Manager.

The work is being administered at the Astronuclear Laboratory by R. T. Begley, with R. W. Buckman, Jr. serving as principal investigator. Other Westinghouse personnel contributing are G. G. Lessmann, Weldability and Thermal Stability, and D. R. Stoner, Oxygen Contamination.

ABSTRACT

Development of dispersion strengthened tantalum base alloys for use in advanced space power systems continued with the completion of a study of the effect of welding, aging, and oxygen contamination on the ductile-brittle transition of six alloys. The alloys evaluated included carbide, nitride, and carbonitride strengthened types, as well as two solid solution alloys. Further processing and more detailed evaluation of alloy ASTAR-811C (Ta-8W-1Re-0.7Hf-0.025C), a fabricable, creep resistant composition, was also carried out. Preliminary test results indicate that a carbonitride strengthened composition was resistant to lithium corrosion at 2000°F.

AUTHOR

I. INTRODUCTION

This, the ninth quarterly progress report on the NASA-sponsored program "Development of a Dispersion Strengthened Tantalum Base Alloy", describes the work accomplished during the period November 20, 1965 to February 20, 1966. The work was performed under Contract NAS 3-2542.

The primary objective of the current phase of this program is the double vacuum arc melting of three compositions in the form of 60-pound, 4-inch diameter ingots. These compositions are to be selected for potential sheet and tubing applications on the basis of their weldability, creep resistance, and fabricability characteristics.

Prior to this quarterly period several promising tantalum alloy compositions were developed[1]. These alloys exhibited good creep resistance at 1315°C (2400°F), while maintaining adequate fabricability and weldability. From these alloys a weldable composition containing a carbide dispersion (Ta-8W-1Re-0.7Hf-0.025C*) was selected and melted as the first 4-inch diameter ingot (heat NASV-20). The bottom portion of this ingot was upset forged and processed to 0.04-inch sheet. Another section was side forged and processed to 0.04-inch sheet and detailed information on processing characteristics was obtained. Evaluation of this sheet was initiated.

During this quarterly period, the scope of work of the contract was amended by NASA to include a study of the effect of welding, aging, and oxygen contamination on the ductile-brittle transition temperature of solid solution, solid solution plus carbide, solid solution plus nitride, and solid solution plus carbonitride strengthened compositions. This study is to be completed prior to the selection of the final two 4-inch diameter alloys. The two solid solution strengthened compositions, Ta-8.5W-1.5Re-1Hf (NASV-19), and Ta-10W-1Re-0.5Hf (NASV-21), were melted and processed to sheet. Evaluation of weld parameters

*This composition designated ASTAR-811C

and post-weld annealing treatments was completed and the evaluation of oxygen contaminated material was completed with the exception of the 1000-hour aging treatment.

Evaluation of ASTAR-811C sheet (heat NASV-20) was also continued, including identification and morphology of the dispersed carbide phases.

II. PROGRAM STATUS

A. WELDABILITY AND THERMAL STABILITY STUDY

During this period, the scope ot the contract was amended by NASA to include the study of the effect of welding, aging, and oxygen contamination on the ductile-brittle transition temperature of the following six compositions:

Heat No.	Nominal Composition (w/o)	Strengthening Additions
NASV-20 (ASTAR-811C)	Ta-8W-1Re-0.7Hf-0.025C	Solid solution plus carbide
NASV-18	Ta-5W-1Re-0.3Zr-0.04N	Solid solution plus nitride
NASV-12	Ta-7.5W-1.5Re-0.5Hf-0.015C -0.015N	Solid solution plus carbide-nitride
NASV-13	Ta-6.5W-2.5Re-0.3Hf-0.01C -0.01N	Solid solution plus carbide-nitride
NASV-19	Ta-8.5W-1.5Re-1Hf	Solid solution
NASV-21	Ta-10W-1Re-0.5Hf	Solid solution

This study, outlined in Figure 1, is to be completed prior to the final selection of the remaining two 4-inch diameter compositions. Sheet material of compositions NASV-12, NASV-13, and NASV-18, was available from 2-inch diameter ingots prepared previously under this contract. The two solid solution strengthened compositions, NASV-19 and NASV-21 were melted as 2-inch diameter ingots.

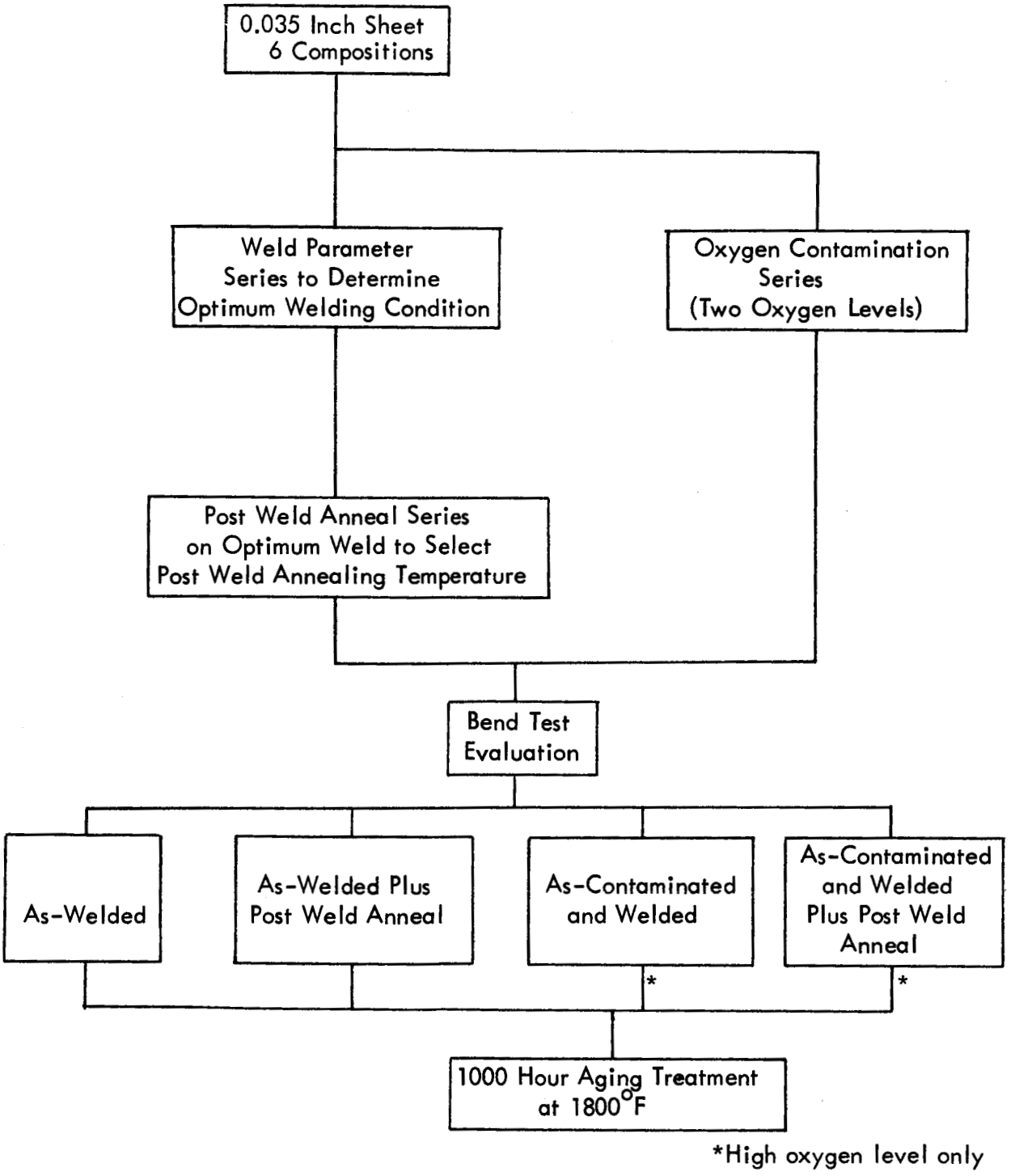

FIGURE 1 - Outline of Weldability and Thermal Stability Program

Melting — Electrodes of compositions NASV-19 and NASV-21 were double vacuum AC arc-melted to provide 2-inch diameter ingots. During the second melt of composition NASV-19, the electrode shorted to the molten pool and froze. A new electrode was assembled from the portion of the ingot that could be salvaged plus a newly assembled length of first melt electrode. This electrode was then double melted. Melting data for compositions NASV-19 and NASV-21 are in Table 1. Both ingots had excellent sidewalls and weighed approximately 7 pounds. Average hardness values of compositions NASV-19 and NASV-21 in the as-cast condition were 272 and 262 VPN respectively.

Primary Breakdown — The 2-inch diameter ingots of NASV-19 and NASV-21 were conditioned, plasma sprayed with molybdenum, and extruded at 1400°C (2550°F) to sheet bar (4:1 reduction ratio). Both extrusions were of excellent quality.

Secondary Working — The extruded sheet bars of compositions NASV-19 and NASV-21 were conditioned, annealed for one hour at 1650°C (3000°F), and cross-rolled to 0.057 inch thick sheet. This sheet was then conditioned, annealed for one hour at 1700°C (3090°F), and rolled to 0.035 inch thick sheet. Yields of rolled sheet ranged from 65 to 70 percent of the conditioned ingot weights.

Chemical Analysis — Chemical analyses results, obtained on compositions NASV-19 and NASV-21, are reported in Table 2. Samples from the bottom of the cast ingots and from 0.035 inch sheet, annealed for one hour at 1650°C (3000°F), were analyzed. A sample from the tail of the extruded sheet bar representing the top of the as-cast ingot of composition NASV-21 was also analyzed. Agreement between intended and analyzed compositions was excellent, and the residual interstitial levels were very low.

Recrystallization Behavior — The one hour recrystallization behavior of compositions NASV-19 and NASV-21 was determined on sections of 0.055 inch thick sheet, which had been reduced 90%. Data are recorded in Table 3. As in the case of the optimization alloys, NASV-12 through NASV-18, these two compositions were fully recrystallized at 1500°C

TABLE 1 - Melting Data for Compositions NASV-19 and NASV-21

Heat No.	Composition	Melt No.	Melt Voltage (volts)	Melt Power (kw)	Melt Rate (lbs/min)
NASV-19	Ta-8.5W-1.5Re-1.0Hf	First	22-23	40-45	2.1
		Second	Electrode shorted to pool		
NASV-19-2[(a)]	Ta-8.5W-1.5Re-1.0Hf	First	24-27	45-50	1.8
		Second	30-33	70-75	3.4
NASV-21	Ta-10W-1Re-0.5Hf	First	22-23	45-50	2.3
		Second	27-28	60-75	4.5

(a) Electrode NASV-19-2 assembled from salvaged portion of second melt electrode plus a section of newly assembled first melt electrode.

(b) Pressure during melting, 5×10^{-4} torr.

TABLE 2 - Chemical Analysis of Compositions NASV-19 and NASV-21

Heat No.	Composition	Position of Sample	Analysis (weight percent) W	Re	Hf	C (ppm)	N (ppm)	O (ppm)
NASV-19	Ta-8.5W-1.5Re-1Hf	Bottom of cast ingot	8.8	1.42	0.97	13	5	---
		Sheet	8.7	1.44	0.99	12	8	13
NASV-21	Ta-10W-1Re-0.5Hf	Bottom of cast ingot	10.0	1.03	0.57	7	3	---
		Top of extruded sheet bar	10.1	1.06	0.54	44	12	---
		Sheet	10.1	1.02	0.54	19	5	15

TABLE 3. Room Temperature Hardness[a], Microstructure[b], and Grain Size[c] of Compositions NASV-19 and NASV-21 After Annealing for One Hour at Temperature

Composition and Heat No.	Prior Reduction (%)	As-Rolled	One Hour Annealing Temperature (°C) / (°F)								
			1200 / 2190	1300 / 2370	1400 / 2550	1500 / 2730	1600 / 2960	1700 / 3090	1800 / 3270	1900 / 3450	2000 / 3630
Ta-8.5W-1.5Re -1Hf(NASV-19)	89.2	363 W	326 W	270 R85	246 R95	245 Rx 0.012	233 Rx 0.017	245 Rx 0.028	244 Rx 0.041	240 Rx 0.068	246 Rx 0.148
Ra-10W-1Re -0.5Hf (NASV-21)	90.0	379 W	336 W	272 R80	252 R90	242 Rx 0.013	242 Rx 0.015	240 Rx 0.023	241 Rx 0.038	241 Rx 0.048	234 Rx 0.078

(a) VPN, 30 Kg load

(b) Microstructure

W - Wrought
R80 - about 80% recrystallized
R85 - about 85% recrystallized
R90 - about 90% recrystallized
R95 - about 95% recrystallized
Rx - fully recrystallized.

(c) Grain size in mm, as determined by standard line intercept method.

(2730°F) with a grain size of 0.012 mm (470μ in.), as determined by the standard line intercept method. Formation of equiaxed grains was 90 to 95% complete after one hour at 1400°C (2550°F).

Base Metal Bend Ductility — The ductile-brittle transition temperature of the base metal of both compositions NASV-19 and NASV-21 was determined to be less than -320°F (<-195°C). Data are recorded in Table 4. Both of these materials also had a minimum room temperature bend radius of zero t, as determined by bending specimens through an angle of 180 degrees (i. e., over on themselves) with no observed fracture.

TABLE 4. Ductile-Brittle Transition Temperature[(a)] of 0.04 Inch Sheet of Compositions NASV-19 and NASV-21

Composition	Temperature		No. Load Bend Angle (Degrees)	Remarks	DBTT	
	°F	°C			°F	°C
Ta-8.5W-1.5Re-1Hf (NASV-19)	-320	-195	94	Bend	<-320	<-195
	-320	-195	95	Bend		
Ta-10W-1Re-0.5Hf (NASV-21)	-320	-195	95	Bend	<-320	<-195
	-320	-195	95	Bend		

(a) Base metal sheet specimens were annealed for 1 hour at 1650°C (3000°F) prior to testing. Bend radius used was 1.8t.

Mechanical Property Evaluation

a. Tensile Properties — Tensile data were obtained at 70,2200, 2400, 2600, and 3000°F (21, 1205, 1316, 1427, and 1650°C) on specimens of compositions NASV-19 and NASV-21 which had been machined from 0.035 inch sheet. Each specimen was annealed for one hour at 1650°C (3000°F) prior to testing. Data are recorded in Table 5. The short time tensile properties of these two compositions are similar to those of ASTAR-811C over the temperature range of room temperature to 2800°F (1538°C).

TABLE 5. Tensile Data on Compositions NASV-19 and NASV-21[a]

Composition and Heat Number[b]	Test Temp. °F	Yield Strength[a]			Ultimate Tensile Strength[a] (psi)	% Elongation		% Reduction in Area
		Upper (psi)	Lower (psi)	0.2% Offset (psi)		Uniform	Total	
Ta-8.5W-1.5 Re-1Hf(NASV-19)	RT	88,000	85,000	86,200	99,500	19.25	32.90	65.60
	2200	--	--	27,400	43,800	--	25.7	--
	2400	--	--	24,900	35,900	--	19.2	--
	2600	--	--	24,500	32,000	--	21.3	--
	3000	--	--	22,000	23,500	--	10.6	--
Ta-10W-1Re-0.5Hf (NASV-21)	RT	82,000	81,600	81,600	96,700	18.95	33.90	58.80
	2200	--	--	25,600	41,200	-	21.9	-
	2400	--	--	23,400	34,300	-	26.9	-
	2600	--	--	23,000	30,000	-	26.6	-
	3000	--	--	20,500	22,100	-	18.2	-

(a) Strain rate of 0.05 in/min throughout test.

(b) Specimens annealed for one hour at 1650°C (3000°F) prior to test.

b. Creep Properties — Creep data for the solid solution alloys NASV-19 and NASV-21 are listed in Table 6. This data is plotted in Figure 2 using the Larson-Miller parameter. Also included on the plot are values for T-111, T-222, and a band which represents the values obtained for the dispersed phase strengthened compositions[2]. The addition of small amounts of rhenium to the Ta-W-Hf matrix results in a significant improvement in creep resistance and confirms earlier observations[1]. The exact strengthening mechanism responsible is not apparent since short time tensile data show no difference between Re and W at the 1 a/o level[6]. Although rhenium additions have a significant effect on creep resistance, the interrelation of the hafnium content and interstitial level in alloys containing interstitial additions is also important as illustrated by the data plotted in Figure 3. Here the stress dependence was evaluated using the relation $\dot{\epsilon}=K\sigma^n$ where $\dot{\epsilon} = 1/t$ where t is the time to 1% strain, K is a constant, and σ is the stress. The stress exponent n is evaluated by the relation $(\frac{\partial \log \dot{\epsilon}}{\partial \log \sigma})_T$. The high value obtained for the constant n for the dispersed phase strengthened alloys is evidence of the effectiveness of the dispersed second phase in impeding dislocation motion. However, detailed discussion of the mechanisms responsible will be deferred to a later report. It is evident that even at 2600°F, the dispersed phase is an effective inhibitor of creep deformation. However, increasing the hafnium content from 0.5 to 1% resulted in serious degradation of the creep resistance at 2600°F. From liquid alkali metal corrosion considerations however, a reactive metal such as hafnium is needed and the detrimental effect of the hafnium on creep resistance can be offset by the interstitial addition.

Weldability and Weld Stability Evaluation

a. Weld Parameter Series — A series of 6 tungsten inert gas (TIG) bead-on-plate welds were made on each of the six compositions listed on page 2 in order to evaluate the effects of welding speed and weld width on the ductile-brittle transition temperature. The weld parameters used are listed in Table 7. For each of the three welding speeds, currents were selected that would result in welds of approximately equal width. The results of the weld parameter study are shown in Table 8. The optimum set of weld parameters selected for use throughout the rest of the weldability and thermal stability program are denoted by asterisks. These optimum sets of parameters were chosen by the type and position of specimen failure where several sets of weld parameters resulted in identical transition temperatures. From the

TABLE 6 - Creep Behavior of Solid Solution Strengthened Tantalum Base Alloys[a]

Specimen	Test Temperature (°C)	Test Temperature (°F)	Stress (psi)	Test Duration (hrs.)	Total Elongation (%)	Time (Hrs.) to Elongate 0.5%	Time (Hrs.) to Elongate 1.0%
Ta-8.5W-1.5Re-1Hf (NASV-19)							
NASV-19-1C	1315	2400	15,400	210.7	1.24	99	180
NASV-19-2C	1315	2400	12,500	239.0	0.48	(250)[b]	(416)[b]
NASV-19-3C	1430	2600	10,000	381.2	5.60	100	160
NASV-19-4C	1430	2600	8,000	232.5	1.49	120	180
Ta-10W-1Re-0.5Hf (NASV-21)							
NASV-21-1C	1315	2400	15,680	209.8	1.83	62	127
NASV-21-3C	1430	2600	10,000	257.7	2.36	130	170
NASV-21-4C	1430	2600	8,000	401.5	1.85	180	284

(a) Specimens annealed for one hour at 1650°C (3000°F) prior to test.

(b) Values in parentheses extrapolated.

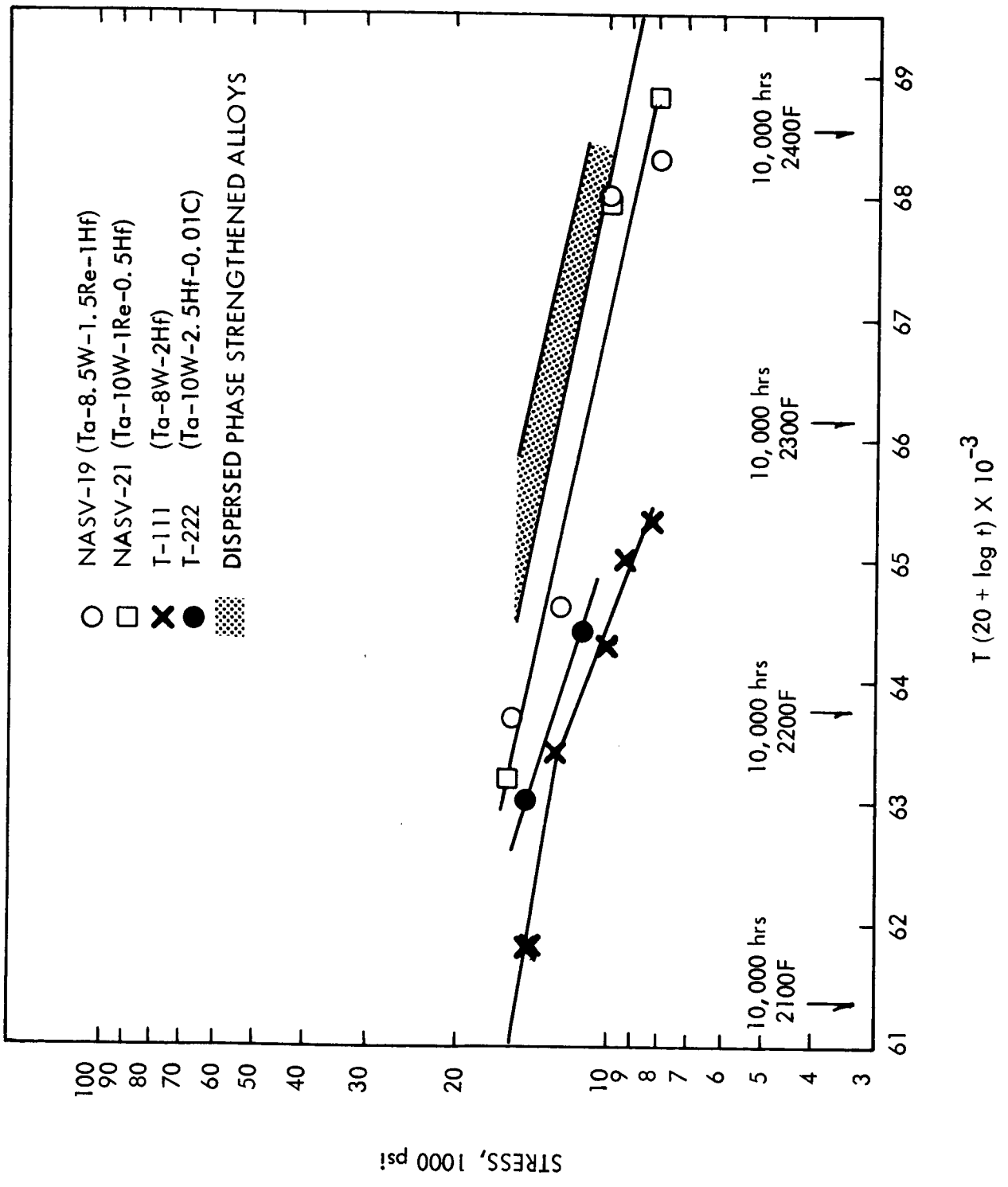

FIGURE 2 - Creep Data for Tantalum Base Alloys (Specimens Annealed for 1 Hour at 1650°C(3000°F) Prior to Test)

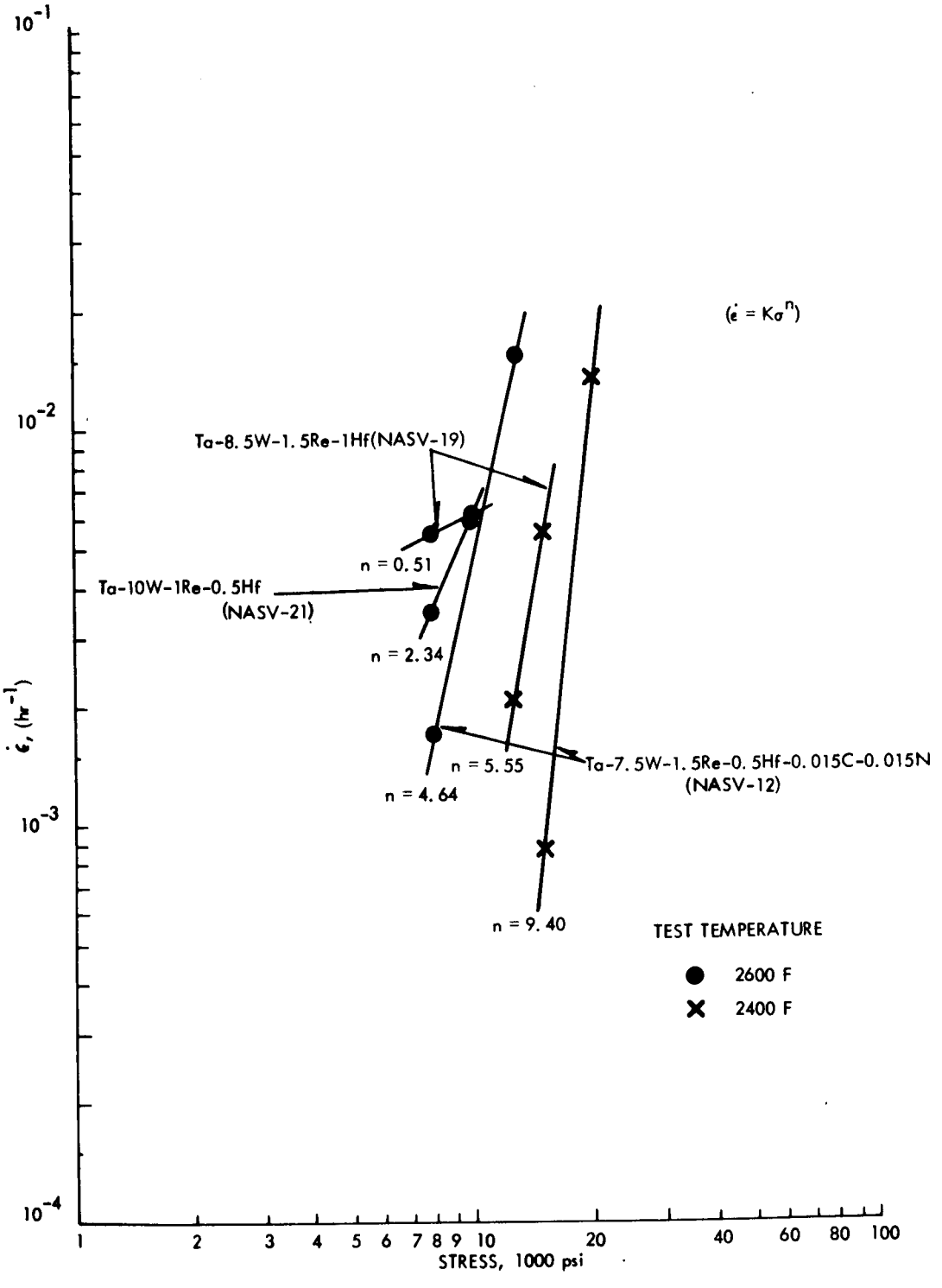

FIGURE 3 - Stress Dependence of Experimental Tantalum Base Alloys (Specimens Annealed for 1 Hour at 1650°C(3000°F) Prior to Test) ($\dot{\epsilon}$ = 1/t where t = time to 1% strain)

TABLE 8. Results of Weld Parameter Study for Compositions NASV-12, NASV-13, 18, 19, 20, and 21.

Composition and Heat Number	Ductile-Brittle Transition Temp.(°F)[c] for Narrow[a] TIG Welds for Welding Parameters of:			Ductile-Brittle Transition Temp.(°F)[c] for Wide[b] TIG Welds for Welding Parameters of:		
	7.5 ipm 76 amps	15 ipm 80 amps	30 ipm 124 amps	7.5 ipm 103 amps	15 ipm 118 amps	30 ipm 158 amps
Ta-7.5W-1.5Re -0.05Hf-0.015C -0.015N (NASV-12)	+100	+100	+100	+75	+125	+125
Ta-6.5W-2.5Re -0.3Hf-0.01C -0.01N (NASV-13)	+75	-125	-200	+100	-150	-175*
Ta-5W-1Re -0.3Zr-0.02N (NASV-18)	-175	-250	-250	-250	-250*	-225
Ta-8.5W-1.5Re -1.0Hf (NASV-19)	-225	-225	-250	-200	-250*	-225
Ta-8W-1Re -0.7Hf-0.025C (NASV-20)	-200	<-250*	<-250	-250	-175	-200
Ta-10W-1Re-0.5Hf (NASV-21)	-175	-225	-250	-200	-225	-250*

(a) Narrow TIG welds taper from 0.100 to 0.140 inches at top to 0.000 to 0.090 inches at bottom.

(b) Wide TIG welds taper from 0.160 to 0.200 inches at top to 0.110 to 0.190 inches at bottom.

(c) Bend test conditions - bend radius 1t, ram speed, 1 inch per minute. DBTT defined as lowest temperature for full 90° bend without evidence of failure.

* Optimum Welding Parameters

data presented in Table 8, it can be seen that the transition temperatures of all six compositions were relatively insensitive to weld width. The transition temperatures were also relatively insensitive to welding speed for all of the compositions except for NASV-13, where increased speeds resulted in significantly increased weld ductility. Because of its response to welding speed, it was also decided to study composition NASV-13 as welded by a non-optimum set of weld parameters for the purpose of comparing the relative effects of post weld annealing.

TABLE 7. Tungsten Inert Gas Weld Parameters for Weldability and Thermal Stability Evaluation of Compositions NASV-12, 13, 18, 19, 20, and 21.

Weld Number	Clamp Spacing (in.)	Welding Speed (ipm)	Welding Current (amps)
1	3/8	7.5	76
2	3/8	7.5	103
3	3/8	15	80
4	3/8	15	118
5	3/8	30	124
6	3/8	30	158

b. Post-Weld Anneal Series — A series of TIG bead-on-plate welds was made on each of the six compositions using the optimum weld parameters determined in the previously discussed weld parameter study. A similar series of welds was also made on composition NASV-13, using the non-optimum weld parameters. All of the welded specimens were then post-weld annealed per the schedule outlined in Table 9. The results of ductile-brittle transition temperature determinations on the post-weld annealed specimens are recorded in Table 10. Compositions NASV-12, NASV-18, NASV-19, NASV-20, and NASV-21 exhibited little or no response to aging. However, composition NASV-13 welded by both sets of weld parameters, exhibited a significant aging response as indicated in Figure 4. These results are in agreement with the results of the weld parameter study where only composition NASV-13

was sensitive to changes in weld parameters. Furthermore, the results of the two-hour post-weld anneals were as expected with respect to aging response (i.e., overaging and the concurrent reduction in transition temperature occurred at a significantly lower temperature and/or shorter time at a given temperature in the material welded using the non-optimum weld parameters where partial aging had already occurred).

TABLE 9. Post-Weld Annealing Schedule for Compositions NASV-12, 18, 19, 20, and 21.

Time (hrs)	Temperatures (°C)	(°F)
2	1200	2190
2	1300	2370
10	1300	2370
2	1400	2550

c. Oxygen Contamination Series — Each of the six compositions was contaminated to two levels of oxygen in order to study the effect of oxygen contamination on their weldability and thermal stability. Contamination levels of 150 ppm and 350 ppm oxygen were chosen from experience with similar tantalum base alloys[2]. These levels were expected to bracket the range of greatest property change with contamination level. The oxidation was accomplished by using a partial pressure of 500 ppm oxygen in ultra pure helium at doping temperatures of 427 to 537°C (800 to 1000°F). An oxygen gage was used on the outlet side of the apparatus to provide an in-process measurement of the amount of oxygen consumed, which was then related to the oxidation rate. The doping temperature was gradually adjusted from 427°C (800°F) to 537°C (1000°F) to maintain an average oxygen weight gain of 20 ppm per hour. Weight gain was used to measure oxygen pickup. The effectiveness of this procedure

TABLE 10. Results of Post-Weld Anneal Study for Compositions NASV-12, 13, 18, 19, 20, and 21

Composition	Weld Speed (ipm)	Parameter Current (amps)	Ductile-Brittle Transition Temperature (°F) for Post Weld Anneals				
			None	2 hrs/2190°F	2 hrs/2370°F	10 hrs/2370°F	2 hrs/2550°F
Ta-7.5W-1.5Re-0.5Hf-0.015C-0.015N (NASV-12)	30	124	<+100	<+175	<0	+200	+75
Ta-6.5W-1.5Re-0.3Hf-0.01C-0.01N (NASV-13)	30	158	-175	+250	+200	0	+150
	7.5	103	+100	+225	-100	+150	-100
Ta-5W-1Re-0.3Zr-0.02N (NASV-18)	15	118	-250	<-175	0	<0	-100
Ta-8.5W-1.5Re-1.0Hf (NASV-19)	15	118	-250	<-320	-250	<-320	<-320
Ta-7W-1Re-0.7Hf-0.025C (NASV-20)	15	80	<-250	<-175	<-200	-200	
Ta-10W-1Re-0.5Hf (NASV-21)	30	158	-250	<-320	<-320	<-320	-250

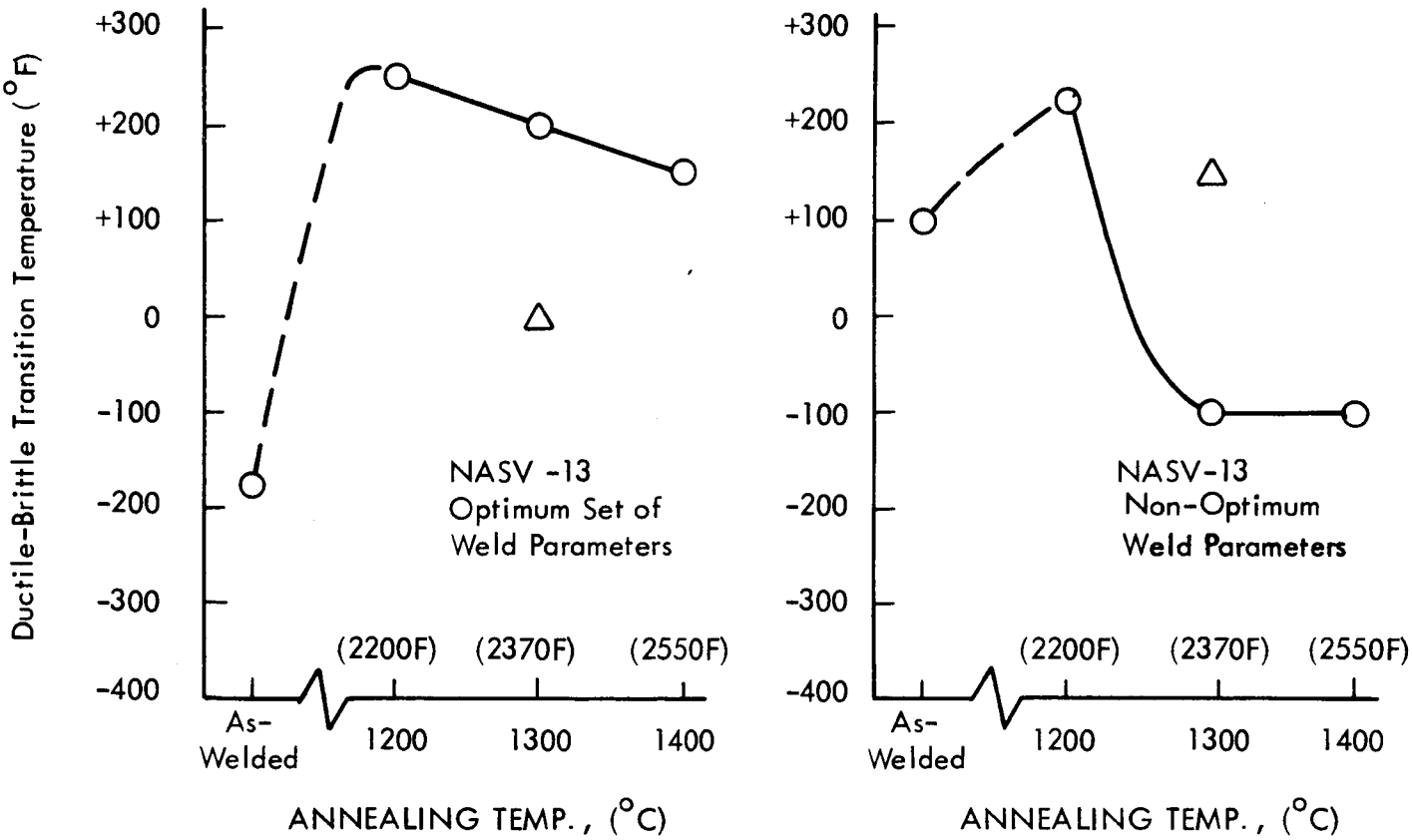

FIGURE 4 - Effects of Post Weld Annealing on the Ductile-Brittle Transition Temperature of NASV-13 (Ta-6.5W-2.5Re-0.3Hf-0.01C-0.01N) (○-2 Hour Post Weld Anneal, △-10 Hour Post Weld Anneal)

has been verified previously by chemical analyses for both oxygen and extraneous contamination[2]. The adherent oxide film produced at the doping temperatures was subsequently diffused into the specimen by annealing for 50 hours at 982°C (1800°F). The apparatus and process control are described in more detail elsewhere[3].

Oxygen contamination data, as determined by weight gain after the 50-hour diffusion anneal, are recorded for the six compositions in Table 11. The low level contamination values (125 to 180 ppm) bracket the desired 150 ppm oxygen value, but the high level contamination values were generally lower than the intended 350 ppm oxygen level, especially for compositions NASV-12, NASV-20, and NASV-21. Chemical analyses of the six compositions (both contamination levels) will be determined to verify the oxygen pickup and to check for nitrogen and carbon contamination.

TABLE 11. Oxygen Content (Calculated) from Weight Gain Data[a] for Compositions NASV-12, 13, 18, 19, 20 and 21

Composition	Oxygen Content	
	Low Level ppm O_2	High Level ppm O_2
Ta-7.5W-1.5Re-0.5Hf-0.015C-0.015N (NASV-12)	130	230 to 305
Ta-6.5W-2.5Re-0.3Hf-0.01C-0.01N (NASV-13)	180	310 to 350
Ta-5W-1Re-0.3Zr-0.02N (NASV-18)	135	240 to 340
Ta-8.5W-1.5Re-1.0Hf (NASV-19)	135	335 to 370
Ta-8W-1Re-0.7Hf-0.025C (NASV-20)	160	245 to 295
Ta-10W-1Re-0.5Hf (NASV-21)	125	205 to 210

(a) After 50 hour/1800°F (982°C) diffusion anneal.

TABLE 12. Bend Transition Results[b] for As TIG Welded Oxygen Contaminated Tantalum Alloy Sheet

Oxygen Level (ppm)	Transition Temperature in °F for								
	NASV-12	NASV-13	NASV-18	NASV-19	NASV-20	NASV-21	T-111[d]	T-222[d]	FS-85[a] [d]
Un-doped[c]	+100	+100	-250	-250	< -250	-250	<-320	-250	-100
125-180	+250	+350	+75	<0	+75	+75	-275	-225	0
205-370	+400	+450	+400		+300	+300	-250	>0	0

(a) Equivalent atomic percent of oxygen

(b) Bend radius 1t

(c) Not subjected to the 50 hour/1800°F (982°C) diffusion anneal

(d) Data from References 2 and 7.

The doped specimens were then TIG welded using the previously determined optimum weld parameters and evaluated for weldability. The results are recorded in Table 12, along with results previously obtained for T-111 (Ta-8W-2Hf), T-222 (Ta-10W-2.5Hf-0.015C), and FS-85 (Cb-27Ta-10W-1Zr). As can be seen, there is a significant increase in transition temperature for all of the compositions as the oxygen content is increased. The failures that occurred during welding of the highly doped NASV-19 material are shown in Figure 5.

B. FOUR INCH DIAMETER INGOT SCALE-UP

Processing and evaluation of ASTAR 811C (Ta-8W-1Re-0.7Hf-0.025C)(heat NASV-20),continued.

Secondary Working — A 18-inch by 6.4-inch by 0.240-inch plate of heat NASV-20 processed from a side forged 4-inch diameter ingot, was annealed for one hour at 1480°C (2700°F) in a vacuum of $< 5 \times 10^{-5}$ torr and then cross rolled to a 0.040-inch thickness at room temperature. The resulting 18-inch by 33-inch sheet is shown in Figure 6. The mottled appearing surface was caused by the hot breakdown rolls used for the cold finishing. Otherwise, the sheet was sound and free of defects. Because the thermal-mechanical history of this sheet differed from the previously evaluated NASV-20 sheet, additional mechanical property and weldability evaluation will be performed on this sheet. This particular sheet has been identified as NASV-20WS.

Recrystallization Behavior — The effect of one hour annealing treatments on the microstructure, hardness, and grain size of ASTAR 811C was determined from 1200 to 2000°C (2192 to 3632°F) on 0.06 and 0.04-inch sheet that had been reduced 73% and 33% respectively. These data are recorded in Table 13. The log of grain size, as determined by the standard line intercept method, is plotted versus the reciprocal of the absolute temperature in Figure 7. The significance of the temperature (1580°C/2850°F) at which the slope of the curve changes is not precisely known, but could be attributed to solution and/or agglomeration of second phase particles.

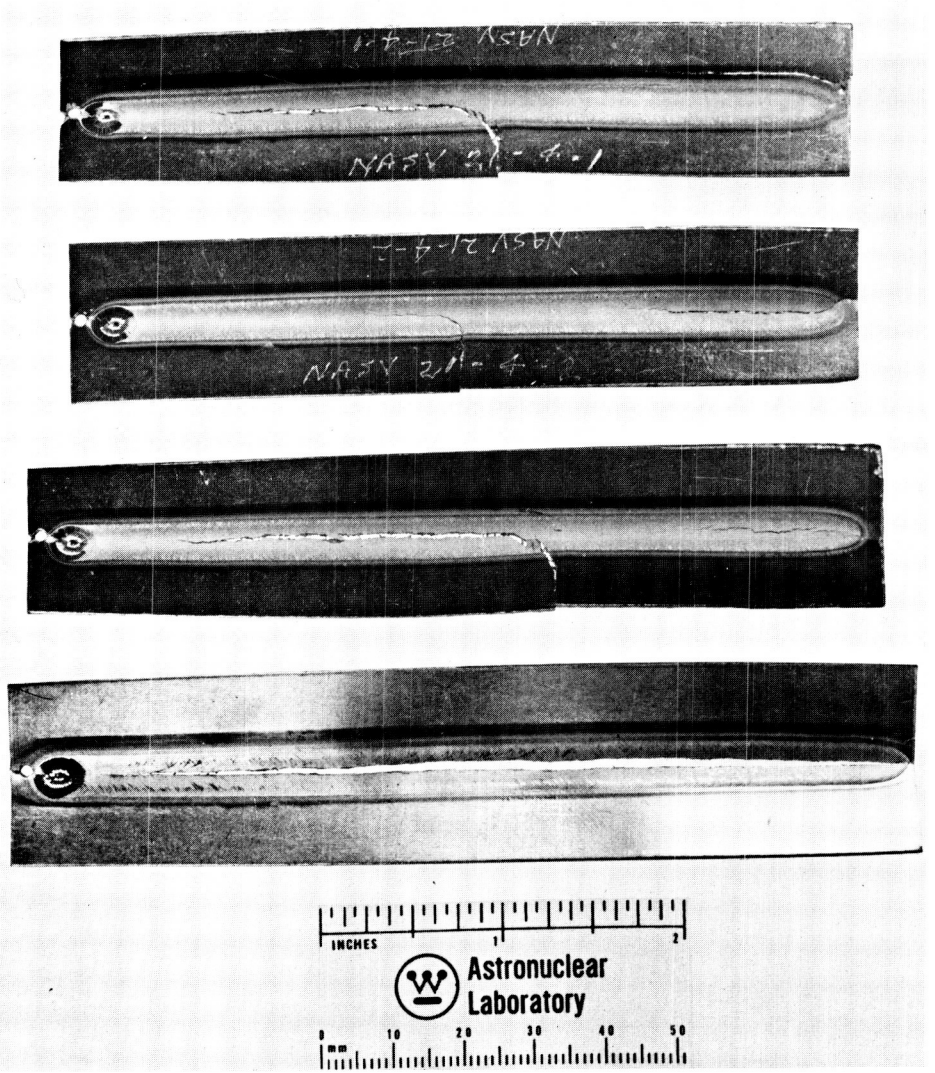

NASV-19
4-1

NASV-19
4-2

NASV-19
5-1

NASV-18
5-2

FIGURE 5. Weld Failures in Compositions NASV-18 and 19 Having a High Oxygen Doping Level

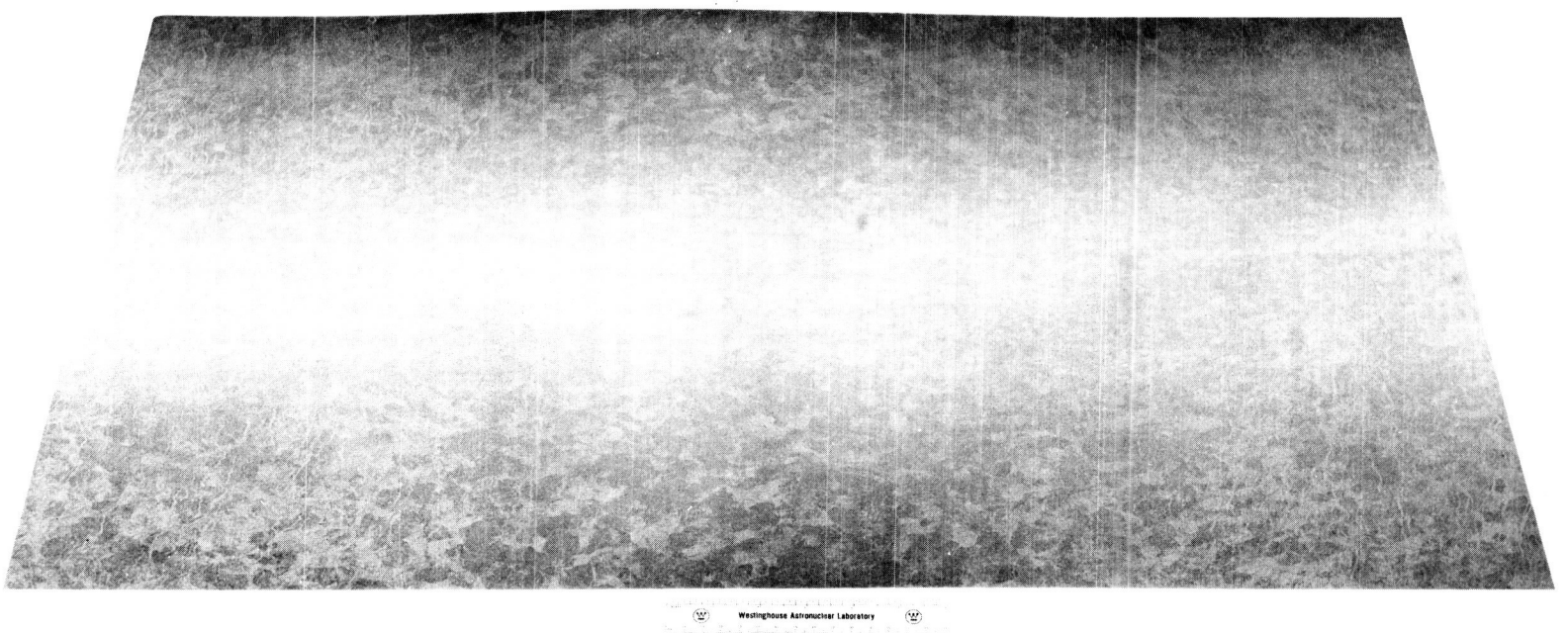

FIGURE 6 - Eighteen Inch by Thirty-Three Inch by 0.04 Inch Sheet of ASTAR-811C (Ta-8W-1Re-0.7Hf-0.025C) (Heat NASV-20)

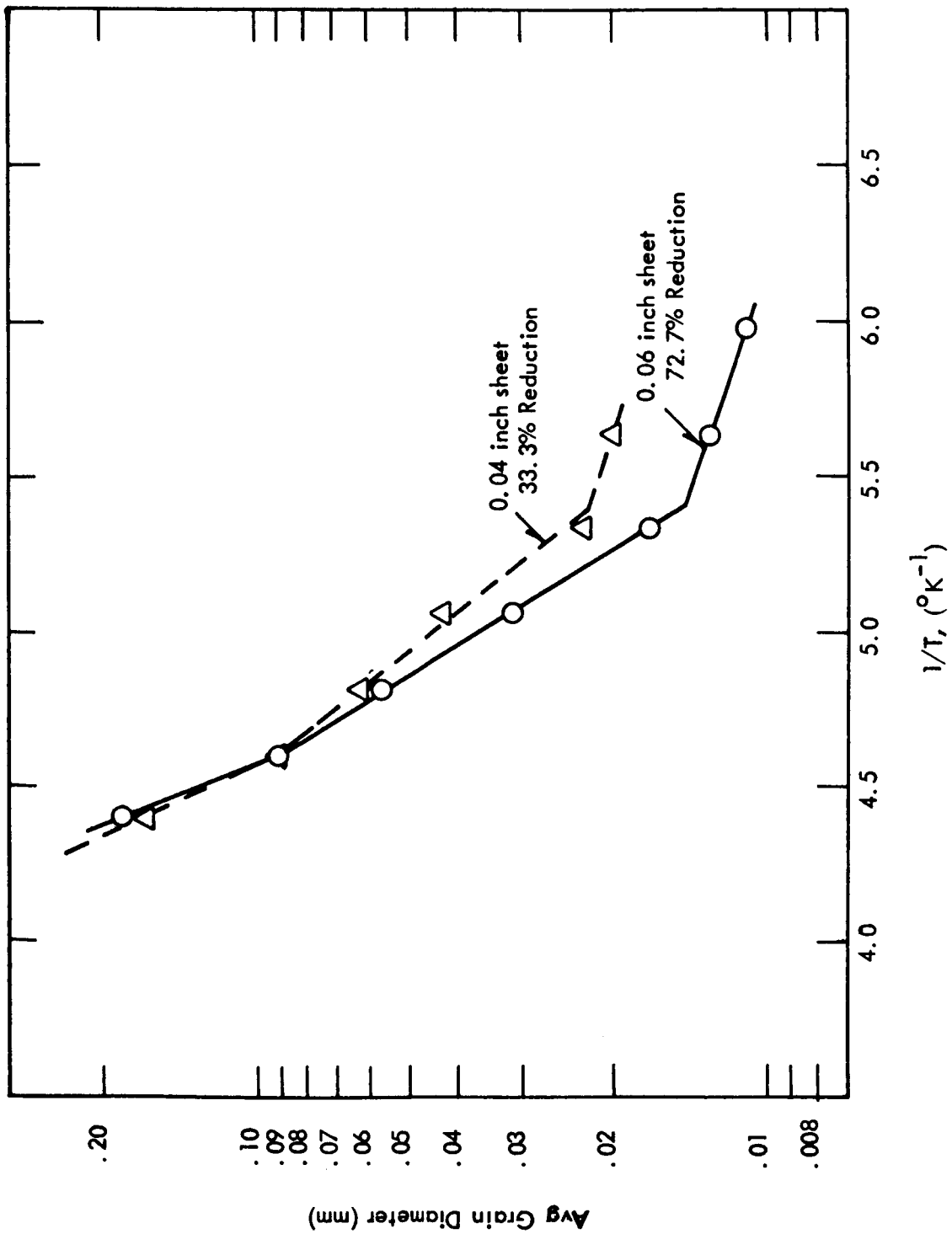

FIGURE 7. One Hour Recrystallization Behavior of ASTAR 811C (Heat NASV-20) (Ta-8W-1Re-0.7Hf-0.025C)

TABLE 13 - Room Temperature Hardness,[a] Microstructure,[b] and Grain Size[c] of As-Rolled ASTAR-811C (Ta-8W-1Re-0.7Hf-0.025C) Sheet[d] After Annealing for One Hour at Temperature

Sheet Thickness	Prior Reduction (%)	One Hour Annealing Temperature (°C) / (°F)									
		As-Rolled	1200 / 2190	1300 / 2370	1400 / 2550	1500 / 2730	1600 / 2910	1700 / 3090	1800 / 3270	1900 / 3450	2000 / 3630
0.04" Sheet	33.3	321	282	283	263	258	254	245	240	248	246
		W	W	W	R_B	R_X	R_X	R_X	R_X	R_X	R_X
		--	--	--	--	0.020	0.023	0.043	0.063	0.091	0.182
0.06" Sheet	72.7	387	319	252	245	263	260	253	253	250	248
		W	R_{50}	R_{90}	R_X	R_X	R_X	R_X	R_X	R_X	R_X
		--	--	--	0.011	0.013	0.017	0.033	0.057	0.091	0.167

(a) VPN, 30 Kg Load

(b) Microstructure
- W - Wrought
- R_B - Recrystallization just beginning
- R_{50} - About 50% recrystallized
- R_{90} - About 90% recrystallized
- R_X - Fully recrystallized

(c) Grain size in mm, as determined by standard line intercept method.

(d) Sheet processed from side forged 4 inch diameter ingot.

Weldability — Bead-on-plate tungsten inert gas welds, made on 0.04-inch and 0.05-inch NASV-20 sheet which had been processed from the side forging and annealed for one hour at 1650°C (3000°F), were examined. Both welds were made using a welding speed of 15 inches per minute and a clamp spacing of 3/8 inch. The microstructure of the two welds were essentially identical. One half of an as-welded transition temperature specimen of the 0.04-inch sheet is shown in Figure 8. Also included in the figure are several high magnification inserts of areas of specific interest. The weld zone and its dendritic structure was quite typical of the tantalum base alloys being studied under this contract. An extremely fine precipitate was observed in some grains at 1500X (see insert A). Appreciable epitaxial grain growth was also observed across the weld-heat affected zone interface.

The heat affected zone, as characterized by the dissolution of the tantalum dimetal carbide precipitates, extended approximately 100 mils into the specimen on either side of the weld. Appreciable grain growth, however, was limited to a zone approximately 35 mils on either side of the weld. A well developed substructure was frequently observed within this area of grain growth (insert B). This substructure has previously been observed in the heat affected zones of T-111 (Ta-8W-2Hf) and T-222 (Ta-10W-2.5Hf-0.01C) tungsten inert gas welds also. The heat affected zone near the base metal was characterized by only partial dissolution of the tantalum dimetal carbide precipitates (insert C).

Hardness traverses were taken across the two specimens. The diamond pyramid hardness profiles, shown in Figure 9, are very similar. Solution of carbon is probably responsible for the increased hardness of the weld metal and heat affected zones. As can be seen, the extent of the total weld plus heat affected zones is very largely controlled by the clamp spacing (i.e., the total width of the weld plus heat affected zones is very close to the 3/8 inch clamp spacing for both specimens, even though the width of the weld in the 0.050-inch sheet is appreciably wider than that in the 0.040-inch sheet). As indicated in Section A, ASTAR 811C does not appear to be subject to aging which significantly impairs low temperature ductility.

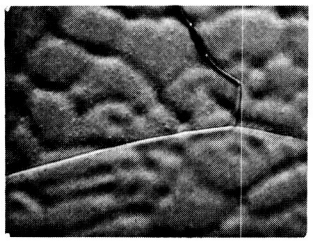

WELD ZONE
1500X

A

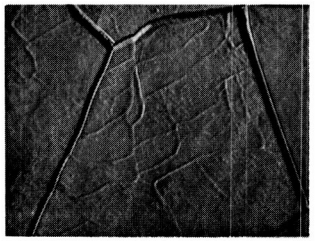

HEAT AFFECTED ZONE
1500X

B

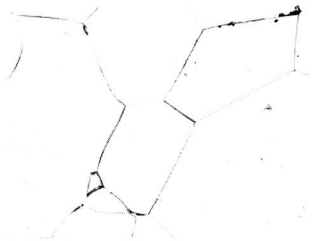

HEAT AFFECTED ZONE
500X

C

FIGURE 8. Microstructure of Tungsten Inert Gas Welds in 0.035-inch Thick ASTAR 811C Sheet
(Reduced 40% for Reproduction)

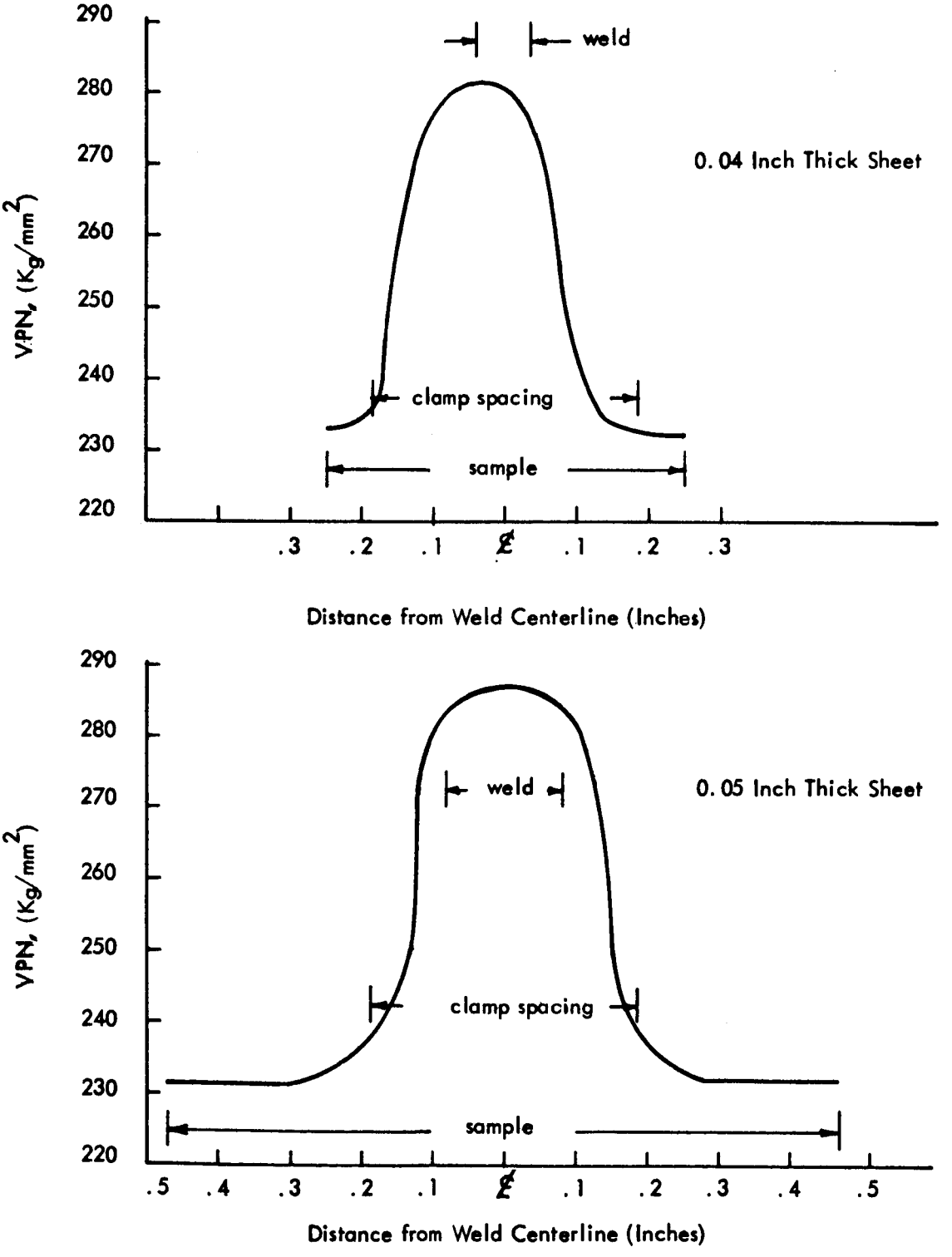

FIGURE 9 - Hardness Traverses of TIG Welded ASTAR 811C (Ta-8W-1Re-0.7Hf-0.025C) Specimens

Mechanical Properties

a. Tensile Properties — Tensile data were obtained on 0.04-inch thick sheet specimens of ASTAR 811C at 816, 1093, 1205, 1427, and 1538°C (1500, 2000, 2200, 2600, and 2800°F). The sheet was processed from the side forging and the specimens were annealed for one hour at 1650°C (3000°F) prior to testing. These data are recorded in Table 14 and in Figure 10, along with the previously obtained tensile data on ASTAR 811C (NASV-20).

Fracture areas from tensile specimens previously tested at -195, 21, 315, and 1315°C (-320, 70, 600, and 2400°F) were metallographically examined. The results are shown in Figure 11. Those specimens tested at the lower temperatures failed predominantly in an intergranular manner even though they exhibited uniform elongations in excess of 15% and total elongations ranging from 24 to 35%. Of special interest is the type of failure exhibited by the specimen tested at -195°C (-320°F), Figure 11a. This failure is similar in appearance to wedge-type intercrystalline fracture as caused by grain boundary sliding at elevated temperature and was not expected. The relative amount of the intergranular failure, apparently associated with the grain boundary carbides, decreased with increasing test temperature.

Bead-on-plate tungsten inert gas welds were made on annealed (one hour at 1650°C/3000°F) 0.05-inch thick NASV-20 sheet to evaluate the effect of welding on room temperature and elevated temperature tensile properties. The weld parameters and resulting microstructure were discussed earlier. The ductile-brittle transition temperature of the as-welded material was determined to be -129°C (-200°F) and is in good agreement with previously obtained data on as-welded 0.04-inch ASTAR 811C sheet. Tensile specimens were machined from the as-welded sheet such that the specimen axis was either parallel or perpendicular to the weld axis. These specimens were then ground to a thickness of 0.04-inch and tested at -195, 21, 982, 1315, and 1427°C (-320, 70, 1800, 2400, and 2600°F). These data are recorded in Table 15 and plotted as a function of temperature in Figure 12. In all cases the welded specimens had higher yield and ultimate strengths than obtained on unwelded specimens while still retaining good ductility. From the earlier microstructural study, which indicated

TABLE 14 - Mechanical Properties of Composition ASTAR-811C[(a)]
(Ta-8W-1Re-0.7Hf-0.025C)

Test Temperature (°F)	Condition	0.2% Yield Strength (psi)	Ultimate Tensile Strength (psi)	% Elongation		% Reduction in Area
				Uniform	Total	
-320	b,d	147,700	165,300	22.05	26.30	41.95
-150	b,d	111,000	130,300	20.05	28.45	46.30
R.T.	b,d	85,000	105,400	16.95	25.90	49.95
R.T.	c,d	85,300	103,500	15.5	26.6	48.40
R.T.	c,e	82,800	104,600	16.35	27.55	49.30
600	b,d	53,700	75,500	15.30	24.45	47.90
1500	b,d	41,300	79,600	---	18.8	---
2000	b,d	35,000	60,900	---	24.0	---
2200	b,d	31,600	49,900	---	28.8	---
2400	c,d	30,400	40,900	---	35.0	---
2600	b,d	29,500	35,300	---	34.8	---
2800	b,d	23,000	28,400	---	49.5	---

(a) Sheet material annealed for 1 hour at 1650°C/3000°F prior to testing.
(b) Material processed from side forging.
(c) Material processed from upset forging.
(d) Strain rate 0.05 in/in/min. throughout test.
(e) Strain rate 0.005 in/in/min. through 0.6% yield and then 0.05 in/in/min. for balance of test.

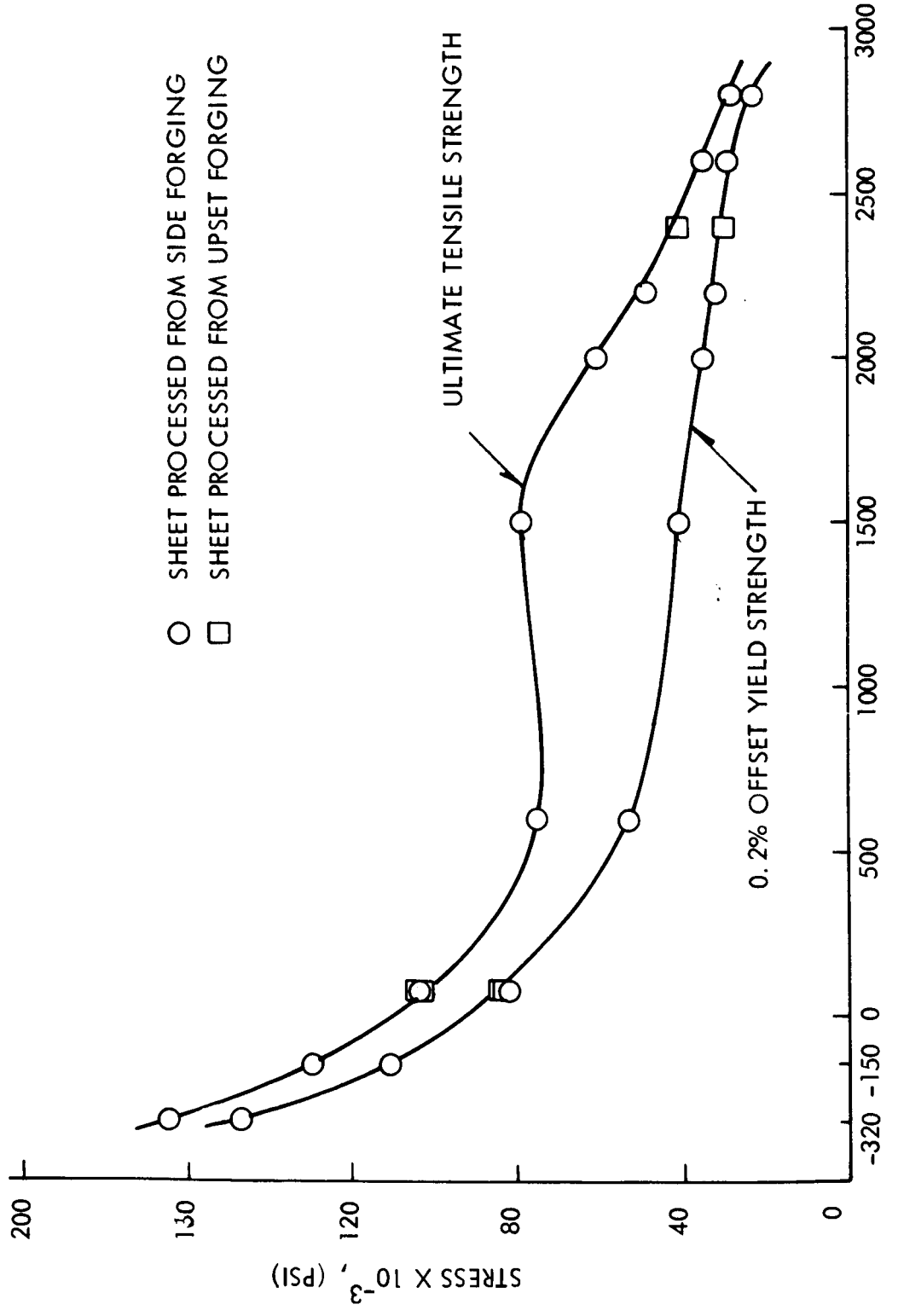

FIGURE 10 - Tensile Properties of ASTAR 811C (Ta-8W-1Re-0.7Hf-0.025C) (Heat NASV-20)

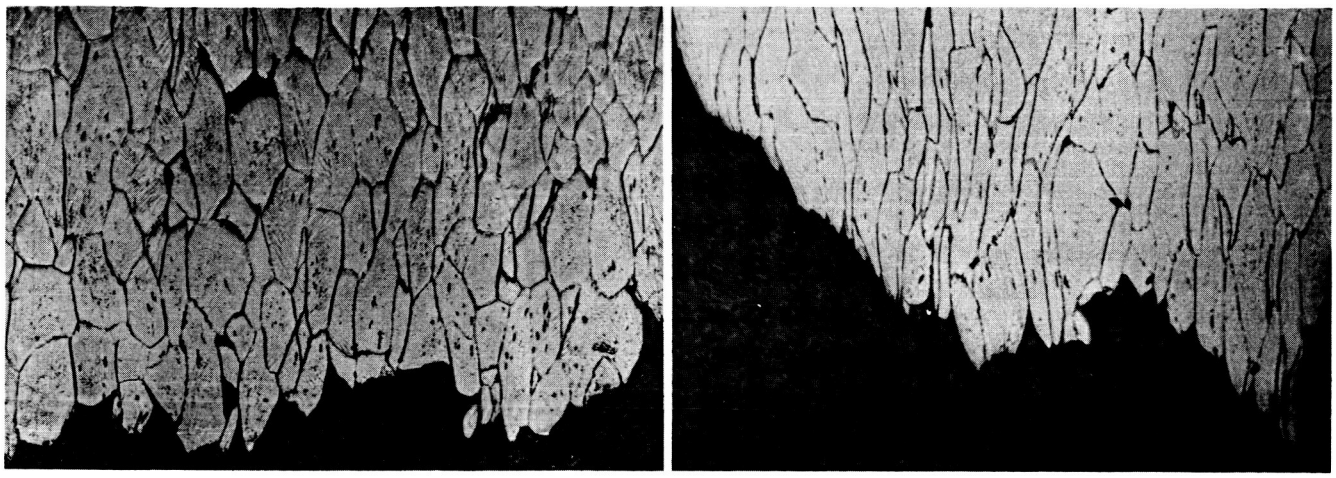

(a) (b)

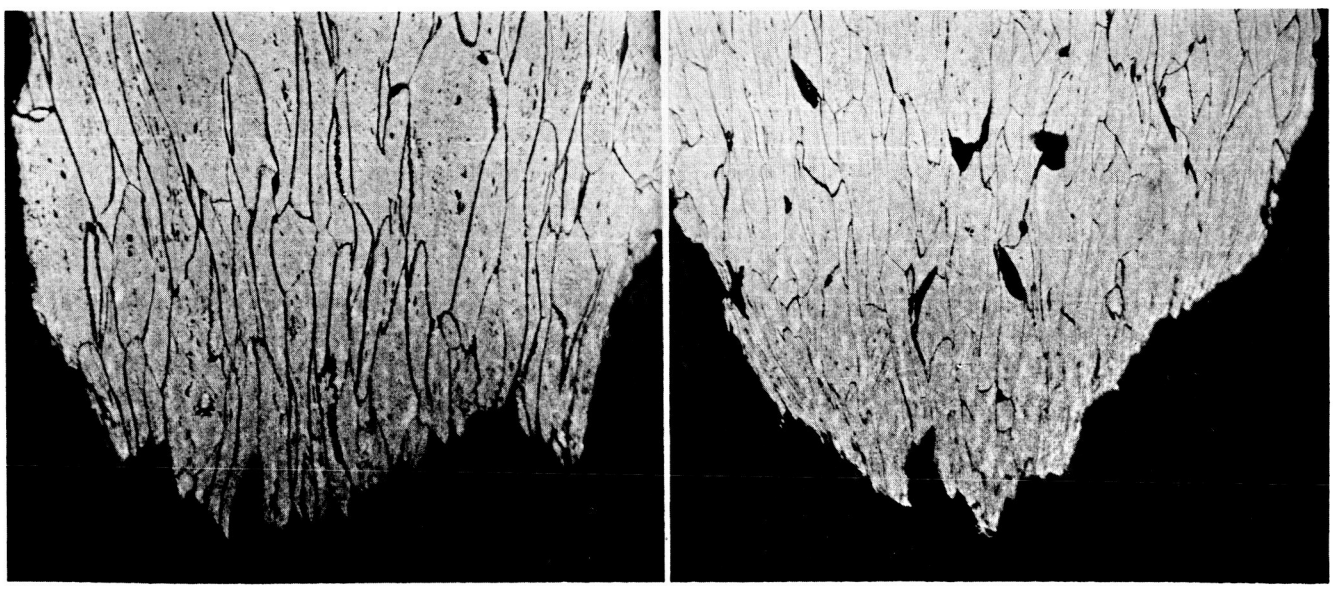

(c) (d)

FIGURE 11. Fracture Characteristics of ASTAR 811C (Ta-8W-1Re-0.7Hf-0.025C) Tensile Specimens Tested at (a) -195°C/-320°F; (b) -101°C/-150°F, (c) 21°C/70°F, and (d) 1315°C/2400°F. 150X

TABLE 15. Tensile Properties of TIG Welded ASTAR 811C[(a)]

Test Temp. (°F)	Weld Direction	0.2% Yield Strength (psi)	Ultimate Tensile Strength (psi)	% Elongation		% Reduction in Area
				Uniform	Total	
-320	Longitudinal	157,300	184,600	16.65	24.20	35.65
-320	Transverse	159,000	176,200	10.90	14.15	41.10
RT	Longitudinal	109,800	115,300	15.0	28.45	48.90
RT	Transverse	89,300	107,200	10.6	18.7	47.8
1800	Longitudinal	44,000	67,100	--	18.7	--
2400	Longitudinal	35,300	41,100	--	29.0	--
2600	Longitudinal	32,500	36,000	--	26.7	--

(a) A constant strain rate of 0.05 inches/minutes used throughout the test.

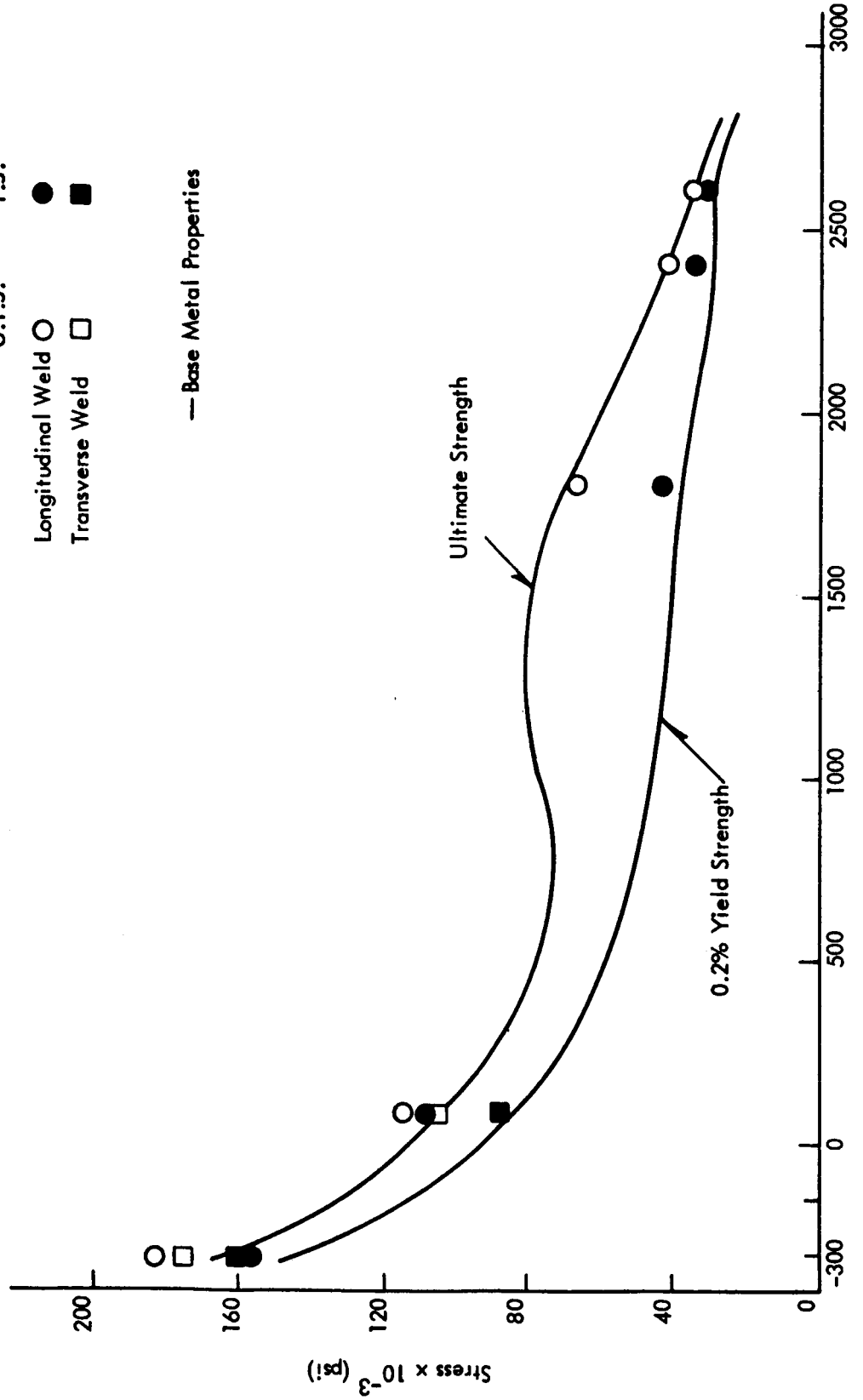

FIGURE 12 - Tensile Properties of TIG Welded ASTAR 811C (Ta-8W-1Re-0.7Hf-0.025C) Specimens

that the width of the weld and heat affected zones were 3/8 inch, it was clear that the entire 1/4 inch wide gage length of the longitudinal welded specimens was composed of weld metal and heat affected metal (i.e., no base metal was contained in the gage length). Thus the increase in strength undoubtedly arises from resolution of carbides in the weld zone during welding. Weld efficiencies of the transverse welded specimens at -195 and 21°C (-320 and 70°F) were 107 and 102% respectively. These increases in strength in the transverse welded specimens are most likely due to the shortening of the effective gage length composed of the weaker base metal. Audible clicks, indicative of twinning, were heard during testing of both the transverse and longitudinal welded specimens at -195°C (-320°F). Indications of twinning were also observed on the stress-strain curves of the two specimens. All of the welded tensile specimens are presently being examined metallographically.

b. Creep Properties — Creep testing of NASV-20 sheet was initiated during this period and the data obtained are listed in Table 16. Creep data on NAS-56 which is an earlier heat having the same composition is also shown and is in good agreement with the present data. Creep tests on ASTAR 811C are scheduled to be run over the temperature range of 2200-2800°F and at stress levels of 4000 to 18,000 psi. The effect of final annealing temperature on the creep resistance will be studied. Specimens of as-TIG welded sheet were machined and will be evaluated during the next period. The weld bead is parallel to specimen axis.

TABLE 16. Results of Creep Tests on ASTAR 811C at 1315°C (2400°F) and at 1×10^{-8} Torr

Prior Treatment	Stress (psi)	Test Duration (hrs.)	Total Elongation (%)	Time(hrs.) to Elongate 0.5%	Time(hrs.) to Elongate 1.0%
Annealed 1 hr at 1650°C (3000°F) [a]	12,500	531	0.03	300	(570) [c]
Annealed 1 hr at 1650°C (3000°F) [b]	12,690	192.6	0.25	(375) [c]	(770) [c]

(a) Data for heat NASV-20
(b) Data for heat NAS-56
(c) Extrapolated

C. PHASE IDENTIFICATION

The identity and morphology of phases present in 0.04 inch ASTAR-811C sheet, processed from the side forging and annealed for one hour at 1650°C (3000°F), was investigated. The microstructure of the sheet is shown in Figure 13. Except for a smaller grain size (0.03 mm), as determined by the standard line intercept method, the microstructure appeared to be quite similar to that of the side forged ingot[5]. As previously observed for heat NASV-20, the residue chemically extracted from the annealed sheet consisted solely of the HCP tantalum dimetal carbide, $(Ta,W)_2C_{1-x}$. The residue was also studied by transmission electron microscopy. Figures 13b and 13c illustrate the general appearance of the precipitates. As in the case of both the as-cast and the side forged ASTAR-811C material, the tantalum dimetal carbides consisted mostly of flower-shaped platelets[5]. However, these platelets were generally smaller than those found in the cast material. The carbide was also observed in the form of very small polyhedra, 0.05 to 0.2μ (Figure 13c) similar to those in the cast material. However, none of the irregular precipitates found in the side forging were present. Thus in spite of the similarity in microstructural appearance with the side forged material, the morphology of the carbide precipitate in the annealed sheet is more nearly similar to that in the cast material.

In order to completely study the morphology of the precipitate occurring within ASTAR-811C, a procedure for producing thin films for transmission electron microscopy was developed. This procedure consists of mechanically thinning specimens to a thickness of 3 to 5 mils by grinding on silicon carbide papers of 120, 240, 320, 400, and finally 600 grit. The specimens are then electro-polished between two stainless steel cathodes in a continuously sitrred electrolyte of 85% H_2SO_4 and 15% Hf, which is maintained at room temperature. A current density of 25 ma/cm results in optimum polishing. Removal of the specimens from the electrolyte for inspection is permissible as long as the voltage is maintained and the anolyte layer is not washed from the specimen surface.

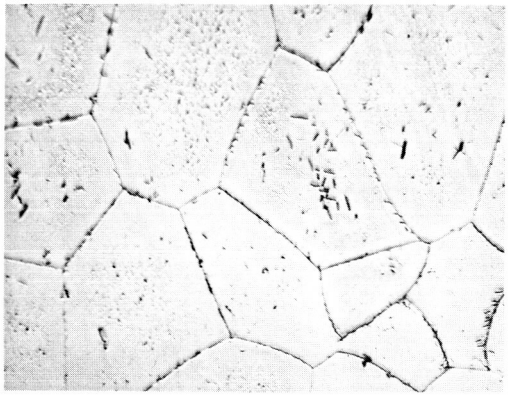

(a) Optical Micrograph 500X

(b) Transmission Electron Micrograph of $(Ta,W)_2C_{1-x}$ Precipitates 10,000X

(c) Transmission Electron Micrograph of $(Ta,W)_2C_{1-x}$ Precipitates 10,000X

FIGURE 13. Optical and Electron Micrographs of Annealed (1 Hr. at 1650°C/3000°F) 0.04 inch ASTAR 811C (Ta-8W-1Re -0.7Hf-0.025C) Sheet

D. ALKALI METAL COMPATIBILITY

The tantalum base alloys developed on this contract are of potential interest for alkali metal containment. However, there has been concern about the use of nitrogen as a strengthener for liquid metal loop systems. The NASA project manager arranged with CANEL (Pratt & Whitney) to evaluate the effects of flowing lithium at 1204°C (2200°F) on the stress rupture properties of the carbonitride strengthened composition NASV-8 (Ta-5.7W-1.56Re-0.7Mo-0.75Hf-0.13Zr-0.015C-0.015N). Of special interest was the stability of the nitrides in the liquid lithium. It was planned to determine the creep rupture properties of the composition in three conditions: 1) after a 1000-hour exposure to liquid lithium at 1204°C (2200°F) in a flowing lithium loop; 2) after a 1000-hour anneal at 1204°C (2200°F) in static argon, and 3) in the as-annealed condition.

The NASV-8 sheet shipped to CANEL had been cold rolled to 0.06-inch thick, annealed for one hour at 1700°C (3092°F), and cold rolled to 0.04-inch thick. The 0.04-inch sheet was then annealed for one hour at 1650°C (3000°F) at CANEL. Initially several specimens were creep rupture tested in Cb-1Zr capsules containing static liquid lithium. Specimen No. 1 was tested at 1204°C (2200°F) under an applied stress of 15,000 psi and specimen No. 2 was tested at 1094°C (2000°F) under an applied stress of 35,000 psi. These tests were suddenly terminated after 243.2 hours and 231.7 hours respectively because of CANEL's shutdown. These two specimens and a third control specimen (No. 3) (in the annealed for one hour at 1650°C/3000°F condition) were returned to Westinghouse for evaluation. A cross section of each specimen's gage length was analyzed for nitrogen content by the Kjeldahl method. The results of the analyses were 0.026, 0.021, and 0.014% nitrogen for specimens 1, 2, and 3 respectively. The nitrogen analysis of the control specimen (No. 3) is in good agreement with the nominal nitrogen content of 0.015 nitrogen. Thus, an appreciable net diffusion of nitrogen into the specimens had occurred. To determine the extent of the existing nitrogen gradient, 15 mils were electropolished* from the cross section of a second piece of the gage length of specimen

*Electropolishing was done in an 85 mil H_2SO_4-15 mil Hf solution at 22°C using a stainless steel cathode, 12-15 volts, and 200-300 ma.

No. 1. Analysis of this specimen indicated a nitrogen content of 0.016% (i.e., just slightly higher than that of the pre-exposure nitrogen level). This result indicated that a large nitrogen gradient existed in the outer 7-1/2 mil surface layer, which had an average nitrogen content of approximately 0.042%. Metallographic examination of the two creep rupture tested specimen's gage sections, however, failed to indicate any differences in microstructure from the surface (Figure 14a) to the center (Figure 14b) due to the nitrogen gradient.

Discussions with CANEL personnel provided no definite explanation of the nitrogen contamination. However, the most probable cause would be loss of cover gas during the sudden shutdown of the whole bank of test equipment. This shutdown consisted of turning off the furnaces and letting the capsule furnaces cool to room temperature, allowing sufficient time for contamination and diffusion to occur. As the source and degree of contamination, and the time-temperature environment during contamination are all uncertain, the results of this evaluation are inconclusive. However, the results do indicate the need for further work in the area of nitrogen stability in nitride strengthened tantalum base alloys having potential use in liquid metal loop systems.

III. FUTURE WORK

During the next quarterly period it is planned to accomplish the following:

1. Continue the creep resistance evaluation of ASTAR 811C.
2. Continue phase identification and morphology studies in detail on composition ASTAR 811C.
3. Establish the compositions of the second and third 4-inch diameter optimized compositions, and initiate electrode fabrication.

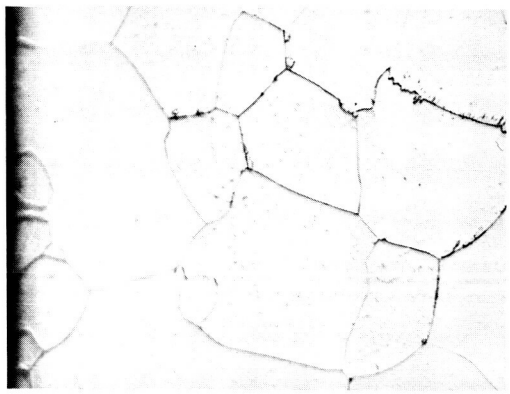

(a) Edge of Specimen

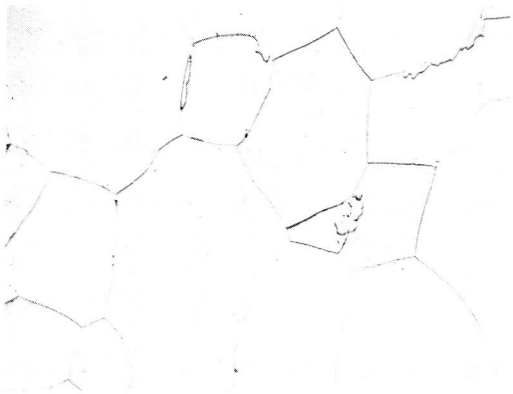

(b) Center of Specimen

FIGURE 14 - Microstructure of Nitride Strengthened NASV-8 (Ta-5.7W-1.56Re-0.7Mo-0.75Hf-0.13Zr-0.015C-0.015N) Creep Rupture Specimen No. 2, Tested for 232 Hrs. Under an Applied Stress of 35,000 psi at 2000°F (1094°C) in Liquid Lithium. 500X
(Etchant - 1 part HNO_3, 1 part HF, 2 parts glycerine)

IV. REFERENCES

1. R. W. Buckman, Jr. and R. T. Begley, Development of Dispersion Strengthened Tantalum Base Alloy, Final Technical Report, Phase I, WANL-PR(Q)-004.

2. G. G. Lessmann and D. R. Stoner, "Determination of the Weldability and Elevated Temperature Stability of Refractory Metal Alloys", 8th Quarterly Progress Report, WANL-PR(P)-008.

3. G. G. Lessmann and D. R. Stoner, "Determination of the Weldability and Elevated Temperature Stability of Refractory Metal Alloys", 7th Quarterly Progress Report, WANL-PR(P)-007.

4. D. R. Stoner (Unpublished Data).

5. R. W. Buckman, Jr., and R. C. Goodspeed, "Development of Dispersion Strengthened Tantalum Base Alloy", 8th Quarterly Progress Report, WANL-PR(Q)-009, NASA-CR-54935.

6. R. W. Buckman, Jr., "Development of Dispersion Strengthened Tantalum Base Alloy", 5th Quarterly Report, NASA-CR-54462.

7. G. G. Lessmann and D. R. Stoner, Determination of the Weldability and Elevated Temperature Stability of Refractory Metal Alloys, 9th Quarterly Progress Report.

DISTRIBUTION LIST

National Aeronautics & Space Administration
Washington, D. C. 20546
Attention: P. R. Miller (RNP)
James J. Lynch (RNP)
George C. Deutsch (RR)
Dr. Fred Schulman (RNP)

National Aeronautics & Space Administration
Scientific & Technical Information Facility
P. O. Box 5700
Bethesda, Maryland 20014
2 copies + 2 reproducibles

National Aeronautics & Space Administration
Ames Research Center
Moffett Field, California 94035
Attention: Librarian

National Aeronautics & Space Administration
Goddard Space Flight Center
Greenbelt, Maryland 20771
Attention: Librarian

National Aeronautics & Space Administration
Langley Research Center
Hampton, Virginia 23365
Attention: Librarian

National Aeronautics & Space Administration
Manned Spacecraft Center
Houston, Texas 77001
Attention: Librarian

National Aeronautics & Space Administration
George C. Marshall Space Flight Center
Huntsville, Alabama 35812
Attention: Librarian

National Aeronautics & Space Administration
Jet Propulsion Laboratory
4800 Oak Grove Drive
Pasadena, California 91103
Attention: Librarian

National Aeronautics & Space Administration
Lewis Research Center
21000 Brookpark Road
Cleveland, Ohio 44135
Attention: Librarian
Dr. Bernard Lubarsky 500-201
Roger Mather 500-309
H. O. Slone 500-201
G. M. Ault 105-1
P. L. Stone 500-201 2 copies
G. M. Thur 500-201
John E. Dilley 500-309
John Weber 3-19
T. A. Moss 500-309
Dr. Louis Rosenblum 106-1
C. A. Barrett 106-1
Report Control Office 5-5

National Aeronautics & Space Administration
Western Operations Office
150 Pico Boulevard
Santa Monica, California 90406
Attention: Mr. John Keeler

National Aeronautics & Space Administration
Azusa Field Office
P. O. Box 754
Azusa, California 91703
Attention: Fred Herrmann

National Bureau of Standards
Washington 25, D. C.
Attention: Librarian

AFSC
Aeronautical Systems Division
Wright-Patterson Air Force Base, Ohio 45433
Attention: Charles Armbruster (ASRPP-10)
T. Cooper
Librarian

Astronuclear Laboratory

Army Ordnance Frankford Arsenal
Bridesburg Station
Philadelphia, Pennsylvania 19137
Attention: Librarian

U. S. Atomic Energy Commission
Germantown, Maryland 20767
Attention: H. Rochen, SNAP 50/SPUR Project Office
Maj. Gordon Dicker, SNAP 50/SPUR Project Office

U. S. Atomic Energy Commission
Technical Information Service Extension
P. O. Box 62
Oak Ridge, Tennessee 37831

U. S. Atomic Energy Commission
Washington, D. C. 20545
Attention: M. J. Whitman

Argonne National Laboratory
9700 South Cass Avenue
Argonne, Illinois 60440
Attention: Librarian

Brookhaven National Laboratory
Upton, Long Island, New York 11973
Attention: Librarian
Dr. D. H. Gurinsky
Dr. J. R. Weeks

Oak Ridge National Laboratory
Oak Ridge, Tennessee 37831
Attention: Mr. J. Devan
Mr. A. Taboada
Mr. H. W. Savage
Librarian

Office of Naval Research
Power Division
Washington, D. C. 20360
Attention: Librarian

Bureau of Weapons
Research and Engineering
Materials Division
Washington 25, D. C.
Attention: Librarian

U. S. Naval Research Laboratory
Washington, D. C. 20390
Attention: Librarian

Aerojet-General Nucleonics
P. O. Box 77
San Ramon, California 94583
Attention: B. E. Farwell

Aerojet-General Corporation
Von Karman Center
Azusa, California 91703
Attention: M. Parkman
R. S. Carey
H. Derow

AiResearch Manufacturing Company
Division of the Garrett Corporation
Sky Harbor Airport
402 S. 36th Street
Phoenix, Arizona 85034
Attention: Librarian
E. A. Kovacevich

AiResearch Manufacturing Company
Division of The Garrett Corporation
9851-9951 Sepulveda Boulevard
Los Angeles, California 90009
Attention: Librarian

IIT Research Institute
10 W. 35th Street
Chicago, Illinois 60616
Attention: Librarian

Babcock & Wilcox Company
Research Center
Alliance, Ohio
Attention: Librarian

North American Aviation, Inc.
Atomics International Division
8900 DeSoto Avenue
Canoga Park, California 91304
Attention: Librarian
J. P. Page
P. B. Ferry

AVCO
Research & Advanced Development Dept.
201 Lowell Street
Wilmington, Massachusetts
Attention: Librarian

Battelle Memorial Institute
505 King Avenue
Columbus, Ohio
Attention: Librarian

DuPont de Nemours Co.
Eastern Lab
Gibbstown, New Jersey
Attention: A. Holtzman
A. Popoff
J. Ransome
K. Mietzner

Electro-Optical Systems, Inc.
Advanced Power Systems Division
Pasadena, California 91107
Attention: Librarian

Fansteel Metallurgical Corporation
North Chicago, Illinois
Attention: Librarian

Philco Corporation
Aeronutronics
Newport Beach, California 92663
Attention: Librarian

General Atomic Division of General
Dynamics Corp, John Jay Hopkins Lab.
P. O. Box 608, San Diego, California 92112
Attention: Librarian

General Electric Company
Flight Propulsion Laboratory Department
Cincinnati, Ohio 45215
Attention: Librarian

General Electric Company
Missile & Space Vehicle Department
3198 Chestnut Street
Philadelphia, Pennsylvania 19104
Attention: Librarian

General Electric Company
Missile & Space Division
Cincinnati, Ohio 45215
Attention: Librarian

General Electric Company
Vallecitos Atomic Laboratory
Pleasanton, California 94566
Attention: Librarian

General Electric Company
Evendale, Ohio 45215
FPD Technical Information Center
Bldg. 100, Mail Drop F-22

General Dynamics/Fort Worth
P. O. Box 748
Fort Worth, Texas
Attention: Librarian

General Motors Corporation
Allison Division
Indianapolis, Indiana 46206
Attention: Librarian

Hamilton Standard
Division of United Aircraft Corporation
Windsor Locks, Connecticut
Attention: Librarian

Hughes Aircraft Company
Engineering Division
Culver City, California
Attention: Librarian

Astronuclear Laboratory

Lockheed Missiles & Space Division
Lockheed Aircraft Corporation
Sunnyvale, California
Attention: Librarian

The Martin Company
Nuclear Division
P. O. Box 5042
Baltimore, Maryland 21203
Attention: Librarian

Martin Marietta Corporation
Metals Technology Laboratory
Wheeling, Illinois

Materials Research Corporation
Orangeburg, New York
Attention: Librarian

Mc Donnel Aircraft
St. Louis, Missouri
Attention: Librarian

MSA Research Corporation
Callery, Pennsylvania 16024
Attention: Librarian

National Research Corporation
70 Memorial Drive
Cambridge, 42, Massachusetts
Attention: Librarian

North American Aviation
Los Angeles Division
Los Angeles, California 90009
Attention: Librarian

United Aircraft Corporation
Pratt & Whitney Aircraft Division
400 Main Street
East Hartford, Connecticut 06108
Attention: Librarian

Republic Aviation Corporation
Farmingdale, Long Island, New York 11735
Attention: Librarian

Solar
2200 Pacific Highway
San Diego, California 92112
Attention: Librarian

Southwest Research Institute
8500 Culebra Road
San Antonio 6, Texas
Attention: Librarian

Superior Tube Company
Norristown, Pennsylvania
Attention: L. Shaheen

TRW, Inc.
23555 Euclid Avenue
Cleveland, Ohio 44117
Attention: Mr. J. J. Owens
Mr. E. J. Vargo
Librarian

Union Carbide Corporation
Stellite Division
P. O. Box 746
Kokomo, Indiana 46901
Attention: Librarian
Technology Department

University of Michigan
Ann Arbor, Michigan 48103
Attention: Dr. R. E. Balshiser

Wah Chang Corporation
Albany, Oregon
Attention: Librarian

Volverine Tube Division
Calcumet and Hecla, Inc.
17200 Southfield Road
Allen Park, Michigan
Attention: Mr. Eugene F. Hill